Water Research 95 (2016) 103–112

Contents lists available at ScienceDirect

Water Research

journal homepage: www.elsevier.com/locate/watres

Efficacy of carbonaceous nanocomposites for sorbing ionizable antibiotic sulfamethazine from aqueous solution

Chen Zhang [a, b], Cui Lai [a, b], Guangming Zeng [a, b, *], Danlian Huang [a, b, **], Chunping Yang [a, b], Yang Wang [a, b], Yaoyu Zhou [a, b], Min Cheng [a, b]

[a] College of Environmental Science and Engineering, Hunan University, Changsha, 410082, PR China
[b] Key Laboratory of Environmental Biology and Pollution Control, Ministry of Education, Hunan University, Changsha, 410082, PR China

ARTICLE INFO

Article history:
Received 1 December 2015
Received in revised form
29 February 2016
Accepted 5 March 2016
Available online 8 March 2016

Keywords:
Sorption
Carbonaceous nanocomposites
Sulfamethazine
Aqueous solution
Aging

ABSTRACT

This paper investigated the key factors and mechanisms of sulfamethazine (SMT) sorption on a novel carbonaceous nanocomposite, and the effects of harsh aging on SMT sorption in the presence and absence of soil and before as well as after aging. The carbonaceous nanocomposites were synthesized by dip-coating straw biomass in carboxyl functionalized multi-walled carbon nanotubes solution and then pyrolyzed at 300 °C and 600 °C in the absence of air. The sorption performance of high temperature carbonaceous nanocomposite on SMT was excellent, as measured sorption distribution coefficient in the order of 10^3–$10^{5.5}$ L kg^{-1}. Carbonaceous nanocomposites were aged either alone or mixed with soil via exposure to nutrients and soil extract (biological aging) or 80 °C for 100 d (chemical aging). No obvious effects of harsh aging on SMT sorption were observed in the presence of soil and/or biological and chemical aging. The primary mechanisms for SMT sorption included partition caused by Van der Waals forces and adsorption caused by hydrogen bonding and π-π electron-donor-acceptor interaction. Comprehensively considering the cost, renewability, and the application to real water samples, the carbonaceous nanocomposites have potential in removal of SMT and possibly other persistent organic pollutants from wastewater.

1. Introduction

Sulfonamide antibiotics are produced in large quantities and heavily used in human therapy and farming industry as veterinary therapeutics and growth promoters (Hirsch et al., 1999; Kim and Carlson, 2007). The antibiotics given to livestock are often poorly metabolized, therefore, residues of sulfonamide compounds end up in environment (surface and groundwater, and finally soil and sediment) (Cheng et al., 2016; Dong et al., 2015; Teixido et al., 2013; Xu et al., 2007). Sulfonamides compete with *p*-aminobenzoic acid to prevent the synthesis of folic acid in bacteria, and thus accelerate the evolution of antimicrobial-resistant bacteria, provoking toxic effect on aquatic species and potentially negative effect on humans (Gao et al., 2012a; Wang et al., 2006). Sulfonamide antibiotics have been detected at concentrations up to 900 mg kg^{-1} in manure, and parts-per-billion levels of sulfonamides in soils, groundwater and adjacent environmental compartments have been reported (Hamscher et al., 2005; Kemper, 2008).

Sulfamethazine (SMT; 4-amino-*N*-[4,6-dimethyl-2-pyrimidinyl] benzenesulfonamide) is an anti-infective agent, and used frequently in the treatment and prevention of infections (e.g., chlamydia, rheumatic fever, urinary tract infections and malaria, etc.) (Gao et al., 2012b). SMT is highly hydrophilic (octanol water partition coefficient: SMT log K_{ow} = 0.27) even in neutral form (predominates between pH 3 and 7), and it is significant to find ways to minimize its runoff, leaching, and bioavailability if entering environmental media is inevitable (Teixido et al., 2011). One way to stabilize the contaminant is to develop efficient, sustainable and economically attractive adsorbents to the contaminated water and soil (Huang et al., 2015; Xu et al., 2012; Zhang et al., 2014b). SMT sorptions have been studied on clay minerals (Gao and Pedersen, 2005), soils (Lertpaitoonpan et al., 2009), organophilic zeolite (Braschi et al., 2010), nano materials (Chen et al., 2015; Qiang et al.,

* Corresponding author. College of Environmental Science and Engineering, Hunan University, Changsha, 410082, PR China.
** Corresponding author. College of Environmental Science and Engineering, Hunan University, Changsha, 410082, PR China.
E-mail addresses: zgming@hnu.edu.cn (G. Zeng), huangdanlian@hnu.edu.cn (D. Huang).

http://dx.doi.org/10.1016/j.watres.2016.03.014
0043-1354/

2013; Yang et al., 2015), biochar (Teixido et al., 2013), steam-activated biochar (Rajapaksha et al., 2015). The sorption capacity of clay minerals and soils cannot meet the needs of the removal of SMT. Zeolite and nano materials exhibit good sorption performance but they are not suitable for large scale application for the cost and potential environmental risk. In comprehensive consideration of the social, economic and environmental benefits, biochar (produced by pyrolysis under limited or no oxygen at moderate temperatures) proposal is feasible, low environmental risk and can be widely implemented large programmes in order to produce effects on global scale (Tan et al., 2015; Zeng et al., 2013a, 2013b).

This revolutionary carbon material extensively exists, and it isn't high-tech, or even novel, and recently the basis for the strong interest in biochar is multi-fold. Complementary and synergistic objectives may motivate biochar applications for soil improvement (for improved agricultural gains as well as the reduced contaminants), energy production, climate change mitigation and waste management (Lehmann and Joseph, 2009; Sparrevik et al., 2014; Titirici et al., 2012). Being a renewable resource, biochar is a promising resource for water, or soil contaminants treatment. Pignatello et al. studied the speciation of SMT on black carbon and the interaction of SMT with biochars of different properties and as a result of weathering in soil (Teixido et al., 2011, 2013). The sorption of SMT onto carbonaceous materials was through multiple mechanisms, such as the electrostatic interactions and the π-π electron donor-acceptor (Chen et al., 2015; Teixido et al., 2011). Hale and coworkers studied the effects of aging (chemical, biological, and physical aging), as well as soil addition on the sorption of pyrene to biochar and activated carbon (Hale et al., 2011). The prerequisite for the application of biochar is a high capacity for pollutant sorption, and is sustained over a long period of time in the presence of soil, especially when exposed to harsh aging environmental conditions. It is significant to enhance the sorption capacity, stability and anti-aging performance of biochar. Recent studies found that carbonaceous nano materials can bind to biochar surfaces (Inyang et al., 2013; Zhang et al., 2014a). Biochar modified by magnetic iron oxide nanoparticles has been used to improve the sorption of heavy metals (Trakal et al., 2016). Biochar was combined with the emerging graphene to create carbonaceous nanocomposites for organic and inorganic pollutants removal (Zhang et al., 2012; Tang et al., 2015). Thus, marrying existing biochar technology with emerging nanotechnology to create hybrid carbonaceous nanocomposites is able to improve the performance of biochar (Inyang et al., 2014). Specific functional groups (carboxyl, hydroxyl, and amine) grafted carbon nanotubes exhibit excellent sorption performance, thermal and chemical stability, and high mechanical strength (Titirici et al., 2015; Tang et al., 2014). However, practical application of carbon nanotubes remains limited for its poor solubility and rapid aggregation in its native state (Inyang et al., 2014; Yan et al., 2015). Utilization of biochar as sorptive supports is able to overcome these limitations, and maintains low-cost while improves the disadvantages of carbon nanotubes and biochar (Beesley et al., 2011; Gong et al., 2009).

Consequently, the goal of the work presented here was to synthesize carbonaceous nanocomposites and test the capacity for SMT sorption. The sorption behavior of SMT to carbonaceous nanocomposites, including the sorption isotherms, mechanisms and the factors potentially affecting the sorption were investigated. Moreover, aging experiments were investigated. Finally, the application of carbonaceous nanocomposites to real SMT wastewater, cost analysis, and renewability evaluation of carbonaceous nanocomposites were also performed.

2. Materials and methods

2.1. Materials

Sulfamethazine (99%, w/w) was purchased from Sigma-Aldrich and its molecular structure, acidity constants, water solubility (Lin et al., 1996; Qiang et al., 2013) and the equilibria between species (Teixido et al., 2011) were shown in Fig. 1. Stock solution (200 mg L^{-1}) was prepared in 1% methanol, and was used to acquire the initial concentrations of SMT in batch sorption studies. Biochar samples were produced from rice straw, which contains approximately 38.1% cellulose, 16.8% hemicellulose and 11.2% lignin according to previous method (Huang et al., 2008, 2010). Carboxyl functionalized short multi-walled carbon nanotubes with diameters ranging from 10 to 20 nm were purchased from the Chengdu Organic Chemicals Co. Ltd. (PR China). All other chemicals were analytical grade and used as received, and all solutions were diluted using ultra-pure water (resistivity of 18.2 MΩ cm).

2.2. Preparation of carbonaceous nanocomposites

Carboxyl functionalized short multi-walled carbon nanotubes (MWCNT) suspensions were prepared by adding 2 g (2% by weight) of MWCNT powder to 100 ml of ultra-pure water, and the MWCNT suspensions were sonicated in an ultrasound homogenizer with an output frequency of 20 kHz for 1 h at pulse intervals of 12 min (Inyang et al., 2014). Rice straw biomass was converted to carbonaceous nanocomposites via a dip-coating procedure (Schoen et al., 2010). MWCNT was coated on rice straw biomass via physical absorption (Van der Waals force, hydrogen bond, and insertion). And the dehydration condensation reaction of amino and carboxyl may be carried out in the process of pyrolysis. Detailedly, dried rice straw was crushed and ground to <1.0 mm in particle size, and 10 g of rice straw powder was added to 100 ml of MWCNT suspensions (stirred for 2 h, 300 rpm). The dried rice straw treated by MWCNT and untreated rice straw were pyrolyzed at 300 °C and 600 °C with a heating rate of 7 °C min^{-1} for 2 h in the absence of air. All carbonaceous materials were rinsed with ultra-pure water three times, and then dried for later use.

2.3. Characterization methods

Elemental compositions (C, H, N and O) of carbonaceous materials were determined by dry combustion, using an elemental analyzer (model EA1110, CE Instruments, Milan, Italy). The pH values of the produced carbonaceous materials were determined in a suspension of solid-to-pure water ratio 1:20 (w/v) using a digital pH meter (Mettler-Toledo, China). The zeta potentials analysis of carbonaceous materials in water solutions was determined with a zeta potential meter (Zetasizer Nano-ZS90, Malvern). The Brunauer-Emmett-Teller (BET) specific surface area and pore volumes were measured by ASAP 2020 Accelerated Surface Area and Porosimetry System (Micromeritics Instrument Corporation, USA). The microstructures of carbonaceous materials were observed by environmental scanning electron microscope (ESEM) (JSM-5600, Japan). Binding energies were conducted based on the X-ray photoelectron spectroscopy (XPS) (Thermo Fisher Scientific-K-Alpha 1063, UK), and the high resolution spectra were calibrated by setting C1s at 284.8 eV. Physiochemical features of carbonaceous materials were investigated via a Renishaw inVia Raman instrument equipped with a cooled silicon charge coupled device detector. Thermogravimetric analysis (TGA) was performed in a stream of air at a heating rate of 10 °C min^{-1} with a Mettler TGA/DSC1 analyzer to test the thermal stability of carbonaceous materials.

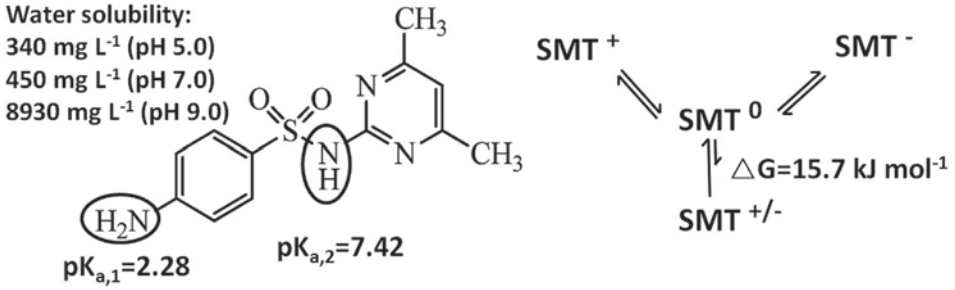

Fig. 1. Molecular structures of sulfamethazine and the equilibria between species.

2.4. Sorption of sulfamethazine

A total of four sorbents including biochar pyrolyzed at 300 °C (BC300), biochar pyrolyzed at 600 °C (BC600), carbonaceous nanocomposites pyrolyzed at 300 °C (BC-MWCNT300), and carbonaceous nanocomposites pyrolyzed at 600 °C (BC-MWCNT600) were used. The sorbents were pre-wetted by flooding with the experimental liquid adjusted to the desired pH for 24 h at 25 °C, then spiked with SMT and other solutes and mixed for an additional 24 h. Methanol was used as a carrier solvent for SMT, and the final methanol concentration was kept below 1% (v/v). NaN_3 (1.5 mM) was used to inhibit aerobic microbial degradation in initial experiments. When applicable, pH was adjusted with HCl or NaOH and ionic strength with NaCl. Sorption isotherms were run with duplicate points for SMT to all sorbents. After spiking with SMT and other solutes, the samples were equilibrated at 150 rpm (25 °C) in an incubator shaker. The samples were then centrifuged at 2000 rpm for 20 min at 25 °C, and the supernatant were filtered using 0.45 μm PVDF disposable filters prior to HPLC analysis (A control, without sorbents, was run for every sample).

2.5. Aging of sorbents

Artificial aging was carried out in the laboratory over 100 d. The two aging regimes used were biological aging and chemical aging. Aging was carried out on BC600 and BC-MWCNT600 alone (100 g), soil alone (500 g) or a mixture of soil and either BC600 and BC-MWCNT600 (500 g with a 5% weight BC600 or BC-MWCNT600 amendment). To ensure a homogeneous soil and sorbents mixture, batches were rolled at 10 rpm for 48 h prior to aging. All batches were maintained at 40% water holding capacity, using either a 1:1 mixture of soil extract: nutrient solution (biological aging) or ultra-pure water (chemical aging). Biological aging consisted of exposing the sorbents to a SMT contaminated soil extract, a nutrient solution containing glucose, peptone, NH_4Cl, KH_2PO_4, $CaCl_2$, $MnSO_4$, $ZnCl_2$, $CuSO_4$ and $MgCl_2$ (Hale et al., 2011). The nutrient solution was added to avoid any limiting environmental conditions and provide an easily degradable C source for microorganisms. Chemical aging was carried out by continually exposing the sorbents to 80 °C in airtight containers. Prior to aging, batches were sterilized to kill native microorganisms.

2.6. Measurement of sulfamethazine concentration

The sulfamethazine concentration in samples was determined using an Agilent HPLC Series 1100 (Agilent, Waldbronn, Germany) equipped with an auto-sampler and a UV–VIS detector. SMT was quantified by UV detection at 268 nm using a Zorbax SB-C18 column (4.6 × 250 mm, 5 μm). The injection volume was 50 μL and the initial eluent flow rate was 1 mL min^{-1}. Mobile phase A was composed of 80% HPLC grade 10 mM acetic acid/ammonium acetate (pH 4.5), and mobile phase B was 20% HPLC grade acetonitrile (Teixido et al., 2013).

3. Results and discussion

3.1. Characterization of carbonaceous nanocomposites

The properties of rice straw biomass substantially changed upon pyrolysis, and the properties of straw biochar pyrolyzed at 300 °C and 600 °C were generally improved by the addition of MWCNT (Table 1). The H/C and (O + N)/C atomic ratios were calculated to evaluate the aromaticity and polarity, respectively (Chen et al., 2008). Relatively lower H/C values of 0.31 and 0.25 for BC600 and BC-MWCNT600, respectively, than BC300 (0.77) and BC-MWCNT300 (0.67), indicated that biochars and carbonaceous nanocomposites produced under high temperature were highly carbonized, and exhibited a highly aromatic structure. In addition, the decrease in (O + N)/C atomic ratio with increasing pyrolysis temperature (from 300 °C to 600 °C) indicated a reduction in the surface polar functional groups (Rajapaksha et al., 2014). The O/C atomic ratio decreased with the increase of pyrolysis temperature (from 300 °C to 600 °C), which indicated that less hydrophilic of carbonaceous materials was produced at 600 °C (Ahmad et al., 2013). The surface areas and pore volume of BC-MWCNT300 and BC-MWCNT600 were significantly improved, and demonstrated MWCNT was anchored to biochars. Furthermore, the microphotographs of BC600 and BC-MWCNT600 were shown in Fig. 2. Amorphous and porous structure of rice straw biochar, and open or closed vesicles (due to the formation and release of volatile components) were observed (Fig. 2a). Accumulated internal pressure with increasing temperature leads to enlargement of internal cavities, coalescence of the smaller pores, and rupturing of various structures (Ahmad et al., 2014; Rajapaksha et al., 2014). As a manifestation, volatile compounds were released. BC-MWCNT600 (Fig. 2c) showed the presence of tubular MWCNT bundles on the surface of biochar, indicating the incorporation of MWCNT in the carbonaceous nanocomposites. According to the analysis of the properties of straw biochar, it was obvious that rice straw pyrolyzed at 600 °C was more suitable for the removal of SMT in aqueous solution due to its physiochemical characteristics.

The XPS C1s peaks of MWCNT, BC600, and BC-MWCNT600 were presented in Fig. 3, which clearly showed that the oxygen containing groups were prevalent on the outer surface of carbonaceous materials. The main peak at 284.8 eV was assigned to aliphatic/aromatic carbon (C–C, C–H, and C=C), then the peaks at 285.9–286.2 eV, 287.3, and 289.8–289.9 eV were attached to the oxygen-containing moieties, that is, C–O, C=O, and O–C=O, respectively. And their relative percentages were listed in Table 2. Fig. 3a showed the preparation of carboxyl groups functionalized MWCNT introduced plenty of hydroxyl groups. Industrial carboxyl/hydroxyl functionalized MWCNT is prepared via oxidation by

Table 1
Proximate and ultimate analysis, surface area and pore volume of rice straw biochar (BC) and MWCNT treated rice straw biochar (BC-MWCNT) produced at 300 and 600 °C.

Sample	Proximate analysis[a]								
	pH			Zeta potential (mV)			Yield (%)		Ash (%)
BC300	6.75 ± 0.03			−29.12 ± 0.74			50.28 ± 0.25		8.32 ± 0.39
BC600	7.32 ± 0.05			−36.35 ± 0.65			33.17 ± 0.40		12.21 ± 0.65
BC-MWCNT300	6.41 ± 0.04			−27.36 ± 0.33			52.11 ± 0.36		7.54 ± 0.56
BC-MWCNT600	6.95 ± 0.05			−33.20 ± 0.85			35.04 ± 0.44		11.62 ± 0.38
Sample	Ultimate analysis								
	C[b] (%)	H[b] (%)	N[b] (%)	O[b] (%)	MolarH/C	MolarO/C	Molar (O + N)/C	Surface area (m^2 g^{-1})	Pore volume (cm^3 g^{-1})
BC300	65.33	4.23	0.81	29.63	0.77	0.34	0.35	2.45	0.005
BC600	83.05	2.15	0.56	14.24	0.31	0.13	0.13	359.42	0.023
BC-MWCNT300	70.14	3.92	0.67	25.27	0.67	0.27	0.28	14.28	0.008
BC-MWCNT600	87.21	1.83	0.51	10.45	0.25	0.12	0.12	387.20	0.286

[a] Mean ± standard deviation (SD) in triplicate determinations.
[b] Elemental compositions and atomic ratios are on an ash-free basis.

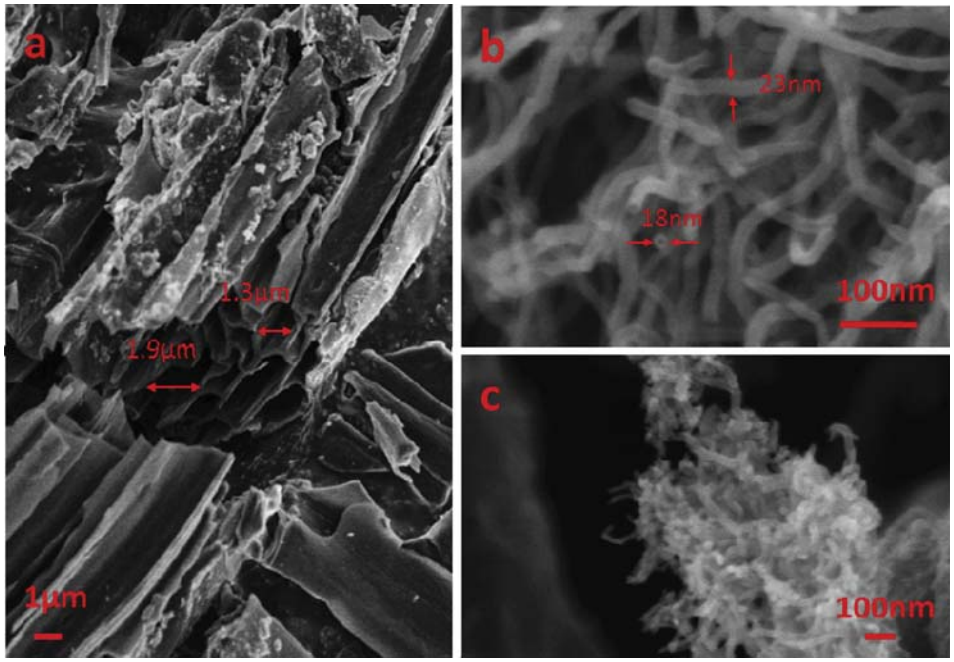

Fig. 2. SEM images of rice straw biochar produced through pyrolysis at 600 °C (a), MWCNT (b), and carbonaceous nanocomposites BC-MWCNT600 (c).

potassium permanganate in different temperatures and different concentrations of sulfuric acid solution. Therefore, the purchased carboxyl groups functionalized MWCNT contains hydroxyl groups frequently. The XPS C1s peaks of BC600 (Fig. 3b) were similar to the reported results of pyrolysis biochar (Fang et al., 2014). The relative percentages of O–C=O were increased due to the introduction of hydroxyl groups functionalized MWCNT for the preparation of carbonaceous nanocomposites.

In Raman spectra (Fig. 4), all carbonaceous materials exhibited two characteristic bands at ~1350 cm^{-1} (D-band) and ~1580 cm^{-1} (G-band) that can be assigned to carbon sp^3 and sp^2 configuration, respectively (Luo et al., 2014). Generally, the D-band originates from defects and functionalities (e.g., −C=O, −OH, and −COOH) within MWCNT walls, and increased I_D/I_G indicated higher defect concentration (increased functional groups) on the sorbents surface (Rajapaksha et al., 2014). The intensity ratios of D- and G-bands (I_D/I_G) were below 1.0 for BC600, indicative of a high graphitization degree of pyrolysis biochar. After incorporating MWCNTs onto BC600, I_D/I_G of BC-MWCNT600 was significantly increased, indicating the increase of functionalities on carbonaceous materials. Thermogravimetric analysis profiles of BC-MWCNT600 exhibited a slightly higher thermal stability due to the introduction of MWCNT (Fig. 5). From 100 to 350 °C, transformation carbon (e.g., aromatic C=C groups) was disappeared, and graphitic chars were formed beyond 350 °C (Chen et al., 2008). Greater weight losses of MWCNT (~94%) and BC-MWCNT600 (~83%) were observed from 350 to 650 °C than BC600 (76%).

3.2. Sorption isotherms

Sorption isotherms of SMT on MWCNT, BC600, and BC-MWCNT600 were presented in Fig. 6. The sorption data were fitted to the Freundlich model:

$$q_a = K_F C_e^n \quad (1)$$

where q_a (mg g^{-1}) is the adsorbed value of adsorbate at equilibrium, C_e (mg L^{-1}) is the equilibrium solute concentration, K_F (mg^{1-n} L^n g^{-1}) is the constant indicative of the relative sorption

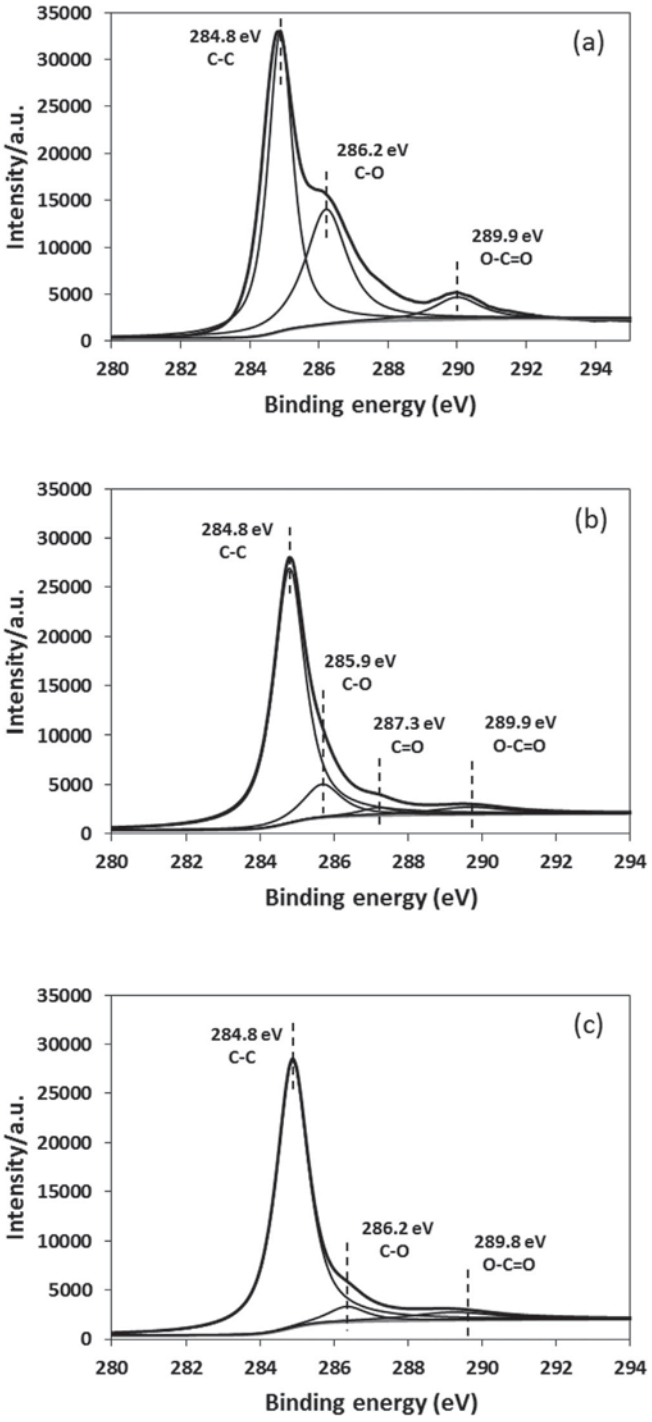

Fig. 3. Deconvolution of XPS C1s for MWCNT (a), BC600 (b), and BC-MWCNT600 (c).

Table 2
C1s bonding state and its relative atomic percentage on MWCNT, BC600, and BC-MWCNT600 as determined by XPS.

Sample	C–C (%)	C–O (%)	C=O (%)	O–C=O (%)
MWCNT	56.09	36.17	N/D[a]	7.74
BC600	79.18	12.67	2.79	5.36
BC-MWCNT600	87.17	5.99	N/D	6.84

[a] XPS analysis showed no presence due to the extremely low content.

capacity of the adsorbent and n (dimensionless) is the exponential

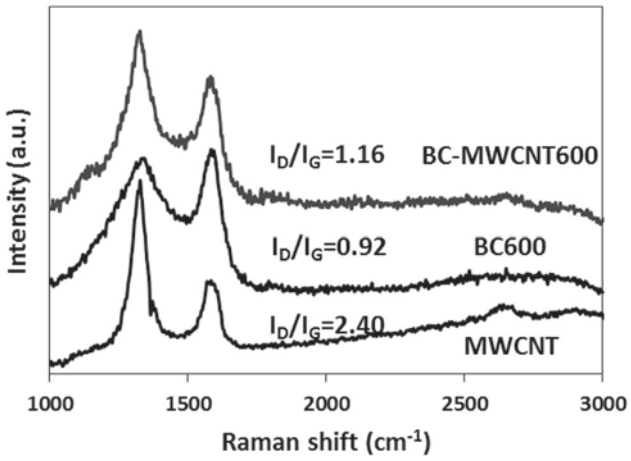

Fig. 4. Reman spectra of MWCNT, BC600, and BC-MWCNT600.

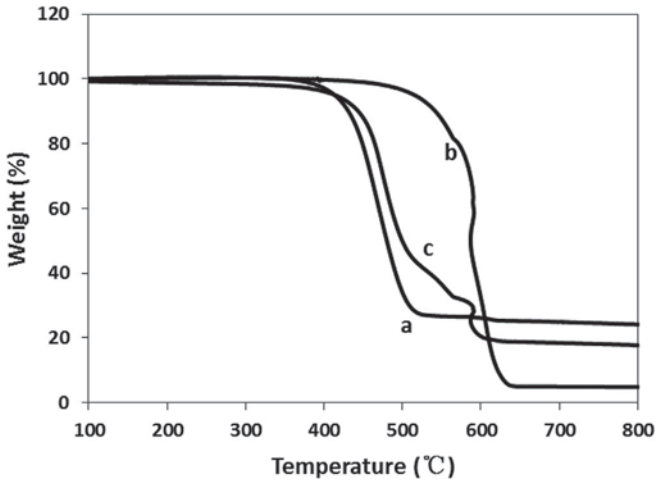

Fig. 5. Thermogravimetric analysis profiles of BC600 (a), MWCNT (b), and BC-MWCNT600 (c).

parameter. The sorption distribution coefficient (K_d, L kg^{-1}) is defined by the ratio of SMT adsorbed per unit sorbent mass (q_a, mg kg^{-1}) and the equilibrium adsorbate concentration (C_e, mg L^{-1}) (Eq. (2)), and V_e (L) is the liquid volume, M_a (kg) is the sorbent mass, C_0 (mg L^{-1}) is the liquid phase concentration without sorbent.

$$K_d = \frac{q_a}{C_e} = \frac{V_e/M_a(C_0 - C_e)}{C_e} = K_F C_e^{n-1} \quad (2)$$

The fitting parameters were summarized in Table 3, and the Freundlich model fits all sorption data reasonably ($R^2 > 0.98$). The sorption affinity could be ordered as follows: MWCNT > BC-MWCNT600 > BC600, and indicated that the introduction of MWCNT created additional sites on the biochar surfaces to facilitate sorption for the large specific surface area and modified functional groups (−OH and −COOH) of MWCNT. Within the tested concentration ranges, the sorption distribution coefficient (K_d) was on the order of 10^3–$10^{5.5}$ L kg^{-1} for SMT on BC-MWCNT600. The observed K_d values are remarkably larger than straw biochar and previously reported costly multiwall carbon nanotubes and graphite (Ji et al., 2009). The mean of reported OC-based distribution coefficients (K_{oc}) from natural soils at pH ~5 was showed in Fig. 6b (Lertpaitoonpan et al., 2009; Teixido et al., 2011). K_{oc} values, given as constants without regard for concentration dependence, are

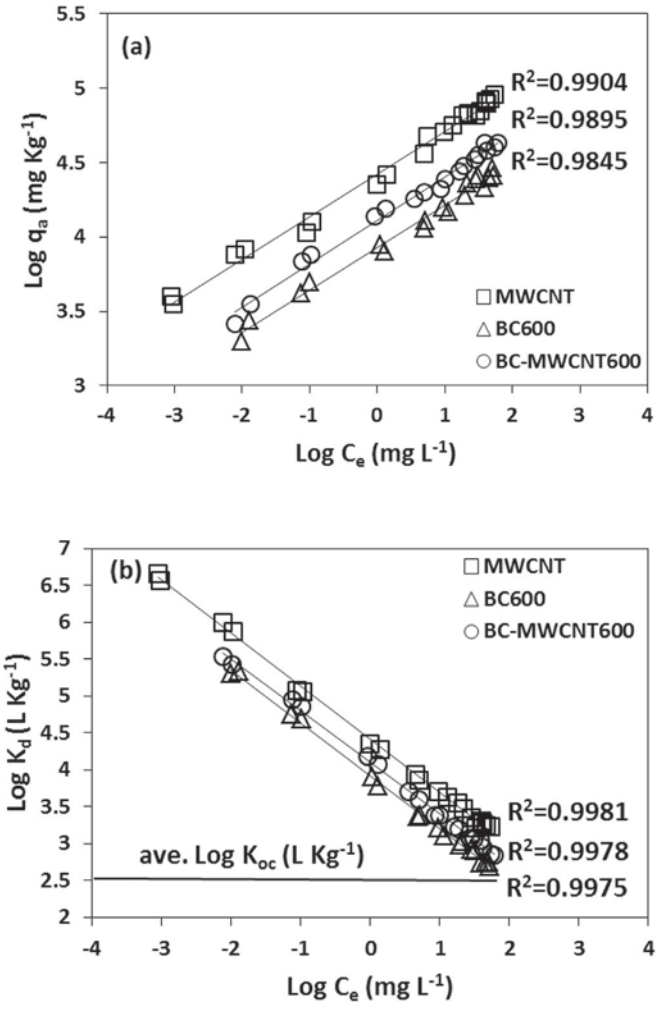

Fig. 6. Sorption isotherms of SMT on MWCNT, BC600, and BC-MWCNT600 at pH = 5.0 plotted as the solid-phase concentration vs equilibrium liquid-phase concentration (a) and plotted as sorption distribution coefficient vs equilibrium liquid-phase concentration (b).

Table 3
Summary of Freundlich model parameters (KF and n ± standard deviation) for sorption to MWCNT, BC600, and BC-MWCNT600.

Adsorbent	K_F ($mg^{1-n} L^n g^{-1}$)	n	R^2
MWCNT	26564.40 ± 662.61	0.2859 ± 0.0066	0.9904
BC600	8446.95 ± 234.65	0.2850 ± 0.0089	0.9845
BC-MWCNT600	12915.17 ± 297.78	0.2913 ± 0.0075	0.9895

calculated assuming all sorption occurs to the OC fraction, and that is they represent an upper limit. The K_d values for the prepared carbonaceous nanocomposites (BC-MWCNT600) lies above the mean K_{oc} all across the isotherm. At the high end of the isotherm (50 mg L^{-1}), K_d is slightly above the mean K_{oc}. And at the low end of the isotherm (10 μg L^{-1}), which more realistically represents environment levels, K_d is ~1000-fold greater than mean K_{oc}. Compared with the K_d values of clay minerals (about 22 L kg^{-1}) (Gao and Pedersen, 2005), tea waste biochars (about 23,000 L kg^{-1}) (Rajapaksha et al., 2014), and functionalized carbon nanotubes (about 14,700 L kg^{-1}) (Zhang et al., 2010), the K_d values of carbonaceous nanocomposites were considerably larger than previously reported values at around pH 5, where SMT^0 predominates.

3.3. Effects of pH on sulfamethazine sorption

The pH influences SMT sorption by changing the surface charge of the sorbents and also the speciation distribution of SMT in solution phase (Wu et al., 2014). The SMT speciation diagram and effects of pH on sorption of SMT to MWCNT, BC600, and BC-MWCNT600 were presented in Fig. 7. The sorption distribution coefficients (log K_d) were nearly constant over the pH range of 3–6 and decreased approximately 30% when the pH increased to 9. The observation implied that MWCNT, BC600, and BC-MWCNT600 exhibited very similar patterns of pH-dependent sorption, suggesting the predominance of graphene surfaces in sorption. The dissociation constant of the sulfonamide group is 7.42 for SMT (see the $pK_{a,2}$ value in Fig. 1), that is the deprotonation begins at pH ~7. The deprotonated anionic form is apparently much less hydrophobic than the protonated neutral counterpart. Moreover, deprotonation on the sulfonamide group would significantly decrease the π-withdrawing ability of the group, therefore suppressing the π-π EDA interaction with the π-donor graphene structure (Ji et al., 2009).

3.4. Effect of ionic strength and humic acid

The presence of salts and humic acid in SMT wastewater may affect the SMT sorption. Therefore, the influence of salt ionic and humic acid strength on the removal of SMT by carbonaceous nanocomposites was studied. Results depicted in Fig. 8a showed that an increase in NaCl concentration also increased SMT uptake slightly. Increasing ionic strength might facilitate sorption of ionic compounds on carbonaceous sorbents, because of the electrostatic screening of the surface charge by the counterion species added (Fontecha-Camara et al., 2007; Vinu et al., 2006). The created hybrid carbonaceous nanocomposites contained −OH and −COOH functionalized MWCNT and straw biochar also contained low surface functionalities, as a result, the increase SMT uptake was reasonable. Moreover, sorption of SMT was dominated by the protonated neutral form (see Fig. 7) where SMT^0 was about 99% (pH 5.0). Therefore, the positive effects of ionic strength on SMT sorption were not significant.

Relatively strong sorption of humic acid on black carbon was reported, and the measured K_d value was 815 ± 38 L kg^{-1} (standard deviation calculated from three replicate samples) for the created hybrid carbonaceous nanocomposites (BC-MWCNT600). The effect of humic acid on the SMT sorption on MWCNT, BC600, and BC-

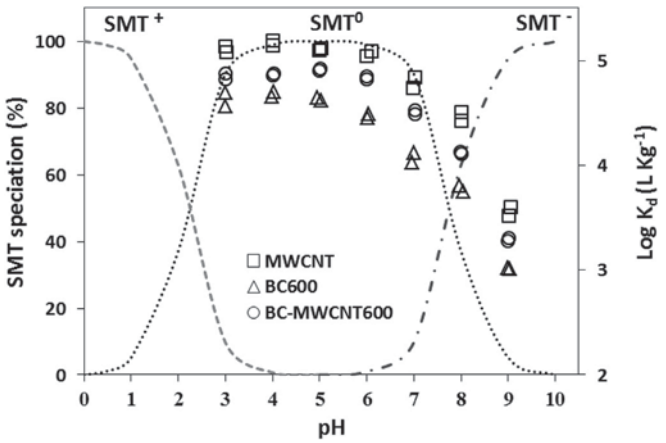

Fig. 7. SMT speciation diagram as a function of pH. And effect of pH on sorption distribution coefficient (log K_d) for duplicate points sorption of SMT on MWCNT, BC600, and BC-MWCNT600.

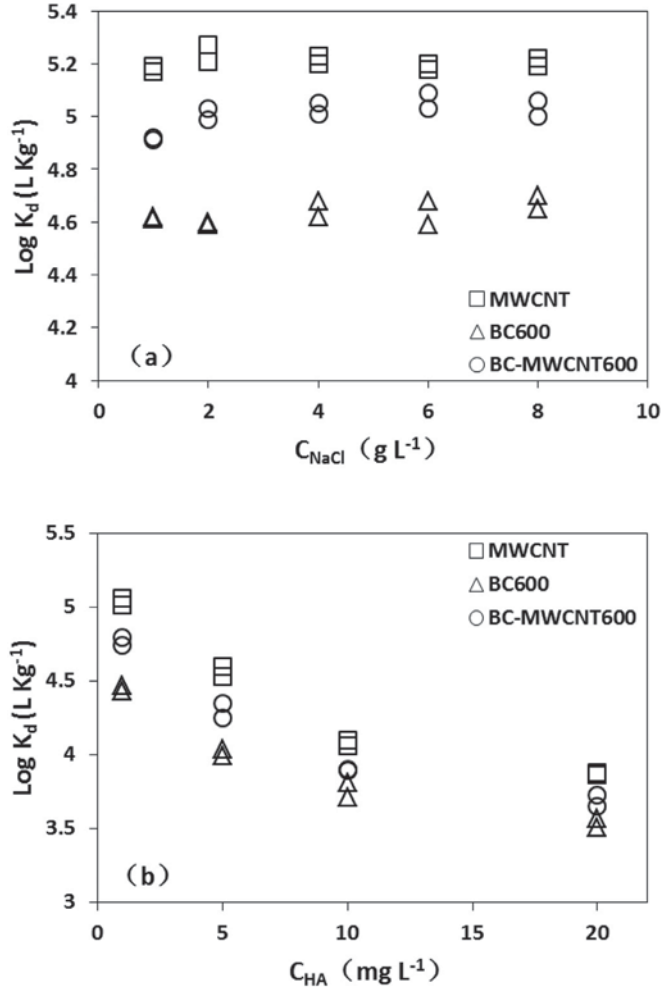

Fig. 8. Effects of ionic strength (a) and humic acid (b) on sorption distribution coefficient (log K_d) for duplicate points sorption of SMT on MWCNT, BC600, and BC-MWCNT600.

MWCNT600 was displayed in Fig. 8b. Changing the humic acid concentration from 1 to 20 mg L^{-1}, sorption of SMT decreased more than a quarter. The suppression caused by humic acid on SMT sorption could be explained by direct competition for sorption sites on carbonaceous sorbents. Due to the obviously larger molecular sizes of humic acid, SMT would be blocked from entering the interstitial spaces of BC-MWCNT600 aggregates and the inner pore spaces to access the sorption sites. Consistently, the suppression of humic acid on SMT sorption on carbonaceous sorbents was negative with adsorbent microporosity, but positive with adsorbate molecular size (Ji et al., 2011; Wang et al., 2009).

3.5. Effect of biological and chemical aging

A high pollutant sorption capacity of the proposed carbonaceous nanocomposites was proved, and its anti-aging performance should also be considered. The sorption strength of BC600 and BC-MWCNT600, with and without soil and before and after aging was quantified by constructing five-point sorption isotherms for SMT. Fig. 9 showed that aging in the manners used here had variable effects on the sorption of SMT by BC600 or BC-MWCNT600 with and without soil. It can be observed that the anti-aging performance of BC600 was improved by introducing the carbonaceous nano materials both in biological aging and chemical aging. The

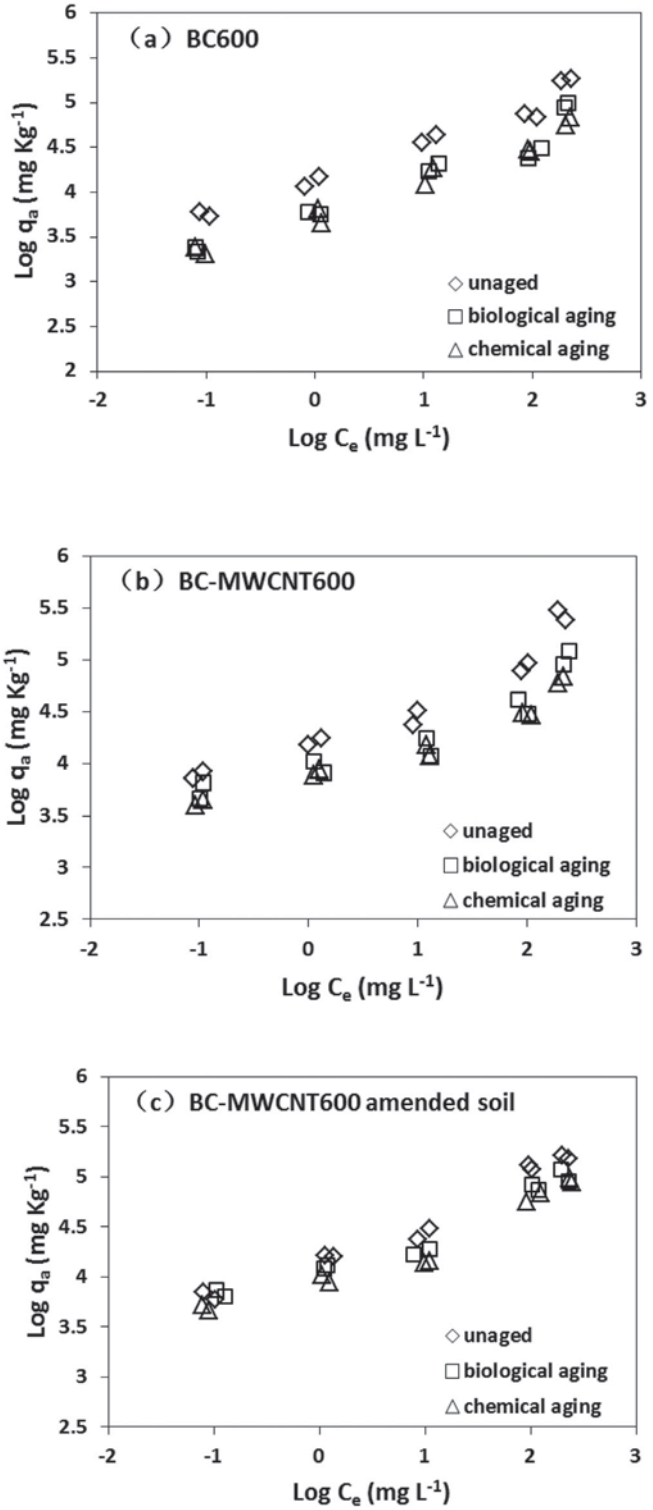

Fig. 9. Sorption isotherms of SMT on BC600 (a), BC-MWCNT600 (b) and BC-MWCNT600 amended soil (c) for unaged, biological aging and chemical aging systems.

sorption of SMT to BC600 decreased about 15%, while the sorption of SMT to BC-MWCNT600 decreased less than 10% at the equilibrium concentration of 1 mg L^{-1}. The biological aging evaluated the influence of dissolved organic matter (DOM) of soil and soil microorganisms on the adsorptivity of the carbonaceous materials. DOM was adsorbed by BC600 and BC-MWCNT600 and thus

occupied the sorbents surfaces and to subsequently reduce the SMT sorption and this was corroborated by the results in Fig. 8b. In addition, carbonaceous materials could be degraded by microorganisms and the hypha might block the inner pores (Yang and Sheng, 2003). However, positive effects of soil microorganisms also occurred, such as biodegradation and microorganism sorption of SMT. Chemical aging altered the physicochemical properties of the sorbents and caused a development of surface functional groups, thus the sorption was not significantly influenced by the creation of some extra exchange sites on the surface of the sorbents (Hale et al., 2011). Fig. 9c indicated that the sorption of SMT to BC-MWCNT600 did not suffer such a great reduction in the presence of soil. And the reduction in the sorption capacity of the carbonaceous nanocomposites was caused by the blockage of pollutant sorption sites by DOM, soil microorganisms, and other anthropogenic contaminants in the soil. The observed limited effects of harsh aging on SMT sorption were not affected to a great extent by the presence of soil and/or biological and chemical aging. Previous study found similar result, where the sorption of simazine to hardwood-derived biochar aged in field for 2 years was the same as that to fresh biochar (Jones et al., 2011).

3.6. Possible mechanisms for SMT sorption

The biochar physicochemical property changes including surface area, pore volume, and surface functional groups occurred in the preparation of carbonaceous nanocomposites, thereby enhancing the sorption efficiency of SMT. BC600 consisted of a large number of micro- (0–2 nm), meso- (2–50 nm) and macropores (>50 nm), and MWCNT (10–20 nm) increased the amount of mesoporous. The SMT molecular size was reported to be 1.050 nm × 0.672 nm (Braschi et al., 2010). Therefore, SMT might diffuse into micro-, meso- and macropores. The primary mechanisms for SMT sorption included partition (caused by Van der Waals forces) and adsorption (caused by hydrogen bonding and π-π electron-donor-acceptor interaction), as illustrated in Fig. 10. For Van der Waals force weakening rapidly with increasing distance, when the adsorbates approach closely to the surface of adsorbents. Hydrogen bonding between the nitrogen of the aniline, sulfinol or pyrimidine group of SMT and the oxygen containing groups (−OH and −COOH) on BC-MWCNT600 was proposed the significant force for SMT sorption. The hydrogen bonding might be strengthened by the condensed aromatic surfaces, since high temperature BC-MWCNT600 provided a hydrophobic microenvironment to accommodate weakly hydrophilic SMT and facilitated the hydrogen bonding to functional groups by the large π subunit of their aromatic substrate (Fang et al., 2014). The delocalized π bond of the aniline group or the pyrimidine ring of SMT could function as a π-electron-acceptor for its electron-withdrawing nature (Qiang et al., 2013). The π-π electron-donor-acceptor (EDA) interaction was also the primary mechanisms governing SMT sorption by carbonaceous nanocomposites. At low pHs, where SMT^+ was predominant, π^+-π electron-donor-acceptor interaction of the protonated aniline ring with electron rich grapheme surfaces of carbonaceous nanocomposites was the important driving force, rather than ordinary cationic exchange reactions (Rajapaksha et al., 2014; Teixido et al., 2011). Under neutral conditions, the K_d values of the sorbents decreased, indicating a partial cation exchange and zwitterionic interactions as the main mechanisms for the sorption of SMT by carbonaceous nanocomposites. And in the alkaline region, the sorption of SMT was partly by proton exchange with water followed by interaction of the resulting neutral molecule augmented. Hydrogen bonding between SMT and a surface phenolate and carboxylate was the dominant mechanism (Teixido et al., 2011). The proposed mechanisms are supported by the pH effects illustrated in Fig. 7. The proposed carbonaceous nanocomposites were weak acidity in aqueous solution, thus promoted the sorption of SMT by reducing the solution pH value. Moreover, acylation reactions may occur between amino group of SMT and carboxyl group of carbonaceous nanocomposites in the presence of a particular catalyst. Overall, BC-MWCNT600 would be a promising sorbent for ionizable antibiotic SMT removal over a broad pH ranges, and it has great potential for the environmental remediation of SMT contaminated water or soils.

3.7. Application of carbonaceous nanocomposites to real water samples

Three different environmental samples, tap water (derived from Changsha Running-water Company), river water (taken from

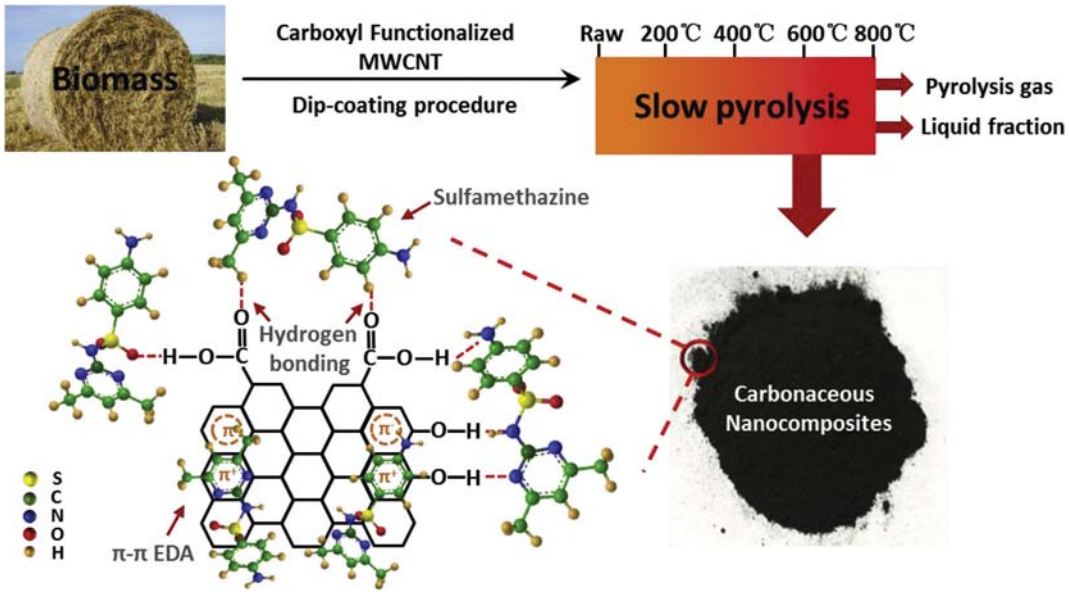

Fig. 10. The formation of carbonaceous nanocomposites (BC-MWCNT600) and proposed mechanisms for SMT sorption.

Dongting Lake, China), and landfill leachate (obtained from municipal solid waste landfills in Changsha, China) samples were used in this study, and the results were shown in Table 4. It was observed that the sorption capacity for SMT in tap water, river water and landfill leachate were less than that in lab ultrapure water. It might be attributed to a higher pH values and the presence of DOM in real water samples. When initial SMT concentration was 10 mg L^{-1}, more realistically representing environment levels, the removal percentage of SMT was more than 90%. The high SMT removal efficiency of carbonaceous nanocomposites indicated the great application potential in removing SMT in real waters.

3.8. The cost analysis and renewability evaluation

The rice straw biomass can be cheaply obtained from agricultural residues. Thus, the cost of BC-MWCNT600 prepared in this work is dramatically affected by the carboxyl functionalized MWCNT consumed and the preparation method. The wholesale price of carboxyl functionalized MWCNT with high purity is approximately US$ 8×10^5 per ton. The pyrolysis and labor cost is estimated to be less than US$ 1000 per ton. Therefore, the cost of carbonaceous nanocomposites is approximately 1.6×10^5 per ton. Comparison with single-walled carbon nanotubes (US$ 441.85×10^6 per ton) (Shawky et al., 2012) and C18 silica (US$ 4×10^6 per ton) (El-Sheikh et al., 2008), the cost of our prepared carbonaceous nanocomposites is much lower. Furthermore, the recyclability is an important factor for evaluating the economy and applicability of sorbents (Wu et al., 2014). The regeneration of BC-MWCNT600 was conducted by adding SMT-loaded BC-MWCNT600 solids to the mixture of methanol and acetic acid (a mass ratio of 10:1) to a final concentration of 500 mg L^{-1} and the mixture was stirred at 25 °C and 150 rpm for 60 min. The results were showed in Fig. 11, after five sorption/desorption cycles, the adsorbed amount of SMT onto the recycled BC-MWCNT600 still remained at 29.95 mg g^{-1}, which only reduced by 8.72% compared to that of the first cycle. The results indicated that the carbonaceous nanocomposites could be a cost-effective, efficient and potential sorbent for SMT removal due to the excellent regeneration performance.

4. Conclusions

A novel sorbent of carbonaceous nanocomposites with excellent sorption capacity is synthesized by dip-coating procedure and slow pyrolysis for the removal of SMT from aqueous solution. The physiochemical properties (surface area, pore volume, thermal stability, sorption capacity and anti-aging performance) of the biochar were enhanced by addition of carboxyl functionalized MWCNT. The distribution ratio K_d at pH 5.0, where SMT^0 was about 99%, was as high as $10^{5.5}$ L kg^{-1}, up to 10^3-fold greater than reported K_{oc}. Moreover, the effects of harsh aging on SMT sorption were not affected to a great extent by the presence of soil and/or aging. The primary mechanisms for SMT sorption included partition caused by Van der Waals forces and adsorption caused by hydrogen bonding and π-π electron-donor-acceptor interaction. The carbonaceous nanocomposites could be a cost-effective, efficient and potential sorbent for environmental remediation of SMT and possibly other persistent organic pollutants from contaminated water or soils.

Table 4
Efficiency of SMT removal by BC-MWCNT600 from real water samples (S/L ratio 1.0 g L^{-1}; contact time 24 h).

Initial SMT concentration in solution (mg L^{-1})	10	50
	q_a (mg g^{-1})	q_a (mg g^{-1})
Ultrapure water (pH 6.0)	9.52	31.42
Tap water (pH 7.0)	9.23	30.05
River water (pH 7.5)	9.08	27.92
Landfill leachate (pH 6.5)	9.24	29.02

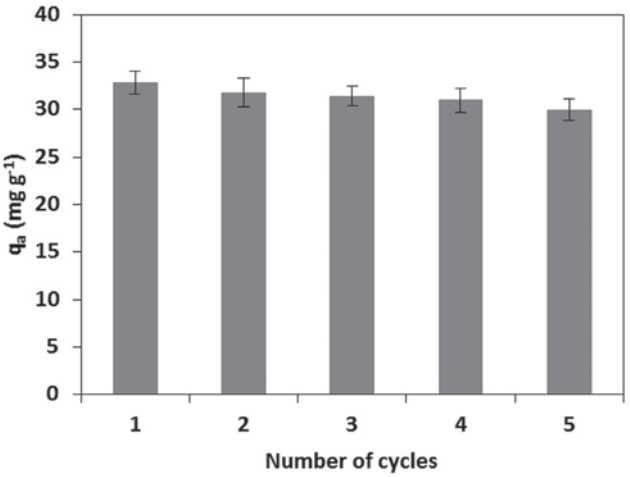

Fig. 11. Reusability of the BC-MWCNT600 for SMT removal (SMT 50 mg L^{-1}; S/L ratio 1.0 g L^{-1}; pH 6.0).

Acknowledgements

This study was financially supported by the National Natural Science Foundation of China (51521006, 51378190, 51278176, 51408206 and 51579098), the Program for New Century Excellent Talents in University (NCET-13-0186), Scientific Research Fund of Hunan Provincial Education Department (521293050), the Program for Changjiang Scholars and Innovative Research Team in University (IRT-13R17), the Fundamental Research Funds for the Central Universities, the Hunan Provincial Innovation Foundation for Postgraduate (CX2015B091), and the International S&T Cooperation Program of China (2015DFG92750).

References

Ahmad, M., Lee, S.S., Rajapaksha, A.U., Vithanage, M., Zhang, M., Cho, J.S., Lee, S.E., Ok, Y.S., 2013. Trichloroethylene adsorption by pine needle biochars produced at various pyrolysis temperatures. Bioresour. Technol. 143, 615–622.
Ahmad, M., Rajapaksha, A.U., Lim, J.E., Zhang, M., Bolan, N., Mohan, D., Vithanage, M., Lee, S.S., Ok, Y.S., 2014. Biochar as a sorbent for contaminant management in soil and water: a review. Chemosphere 99, 19–33.
Beesley, L., Moreno-Jimenez, E., Gomez-Eyles, J.L., Harris, E., Robinson, B., Sizmur, T., 2011. A review of biochars' potential role in the remediation, revegetation and restoration of contaminated soils. Environ. Pollut. 159 (12), 3269–3282.
Braschi, I., Blasioli, S., Gigli, L., Gessa, C.E., Alberti, A., Martucci, A., 2010. Removal of sulfonamide antibiotics from water: evidence of adsorption into an organophilic zeolite Y by its structural modifications. J. Hazard. Mater. 178 (1–3), 218–225.
Chen, B.L., Zhou, D.D., Zhu, L.Z., 2008. Transitional adsorption and partition of nonpolar and polar aromatic contaminants by biochars of pine needles with different pyrolytic temperatures. Environ. Sci. Technol. 42 (14), 5137–5143.
Chen, H., Gao, B., Li, H., 2015. Removal of sulfamethoxazole and ciprofloxacin from aqueous solutions by graphene oxide. J. Hazard. Mater. 282, 201–207.
Cheng, M., Zeng, G., Huang, D., Lai, C., Xu, P., Zhang, C., Liu, Y., 2016. Hydroxyl radicals based advanced oxidation processes (AOPs) for remediation of soils contaminated with organic compounds: a review. Chem. Eng. J. 284, 582–598.
Dong, H.R., Zeng, G.M., Tang, L., Fan, C.Z., Zhang, C., He, X.X., He, Y., 2015. An overview on limitations of TiO_2-based particles for photocatalytic degradation of organic pollutants and the corresponding countermeasures. Water Res. 79, 128–146.
El-Sheikh, A.H., Sweileh, J.A., Al-Degs, Y.S., Insisi, A.A., Al-Rabady, N., 2008. Critical evaluation and comparison of enrichment efficiency of multi-walled carbon nanotubes, C18 silica and activated carbon towards some pesticides from environmental waters. Talanta 74 (5), 1675–1680.

Fang, Q.L., Chen, B.L., Lin, Y.J., Guan, Y.T., 2014. Aromatic and hydrophobic surfaces of wood-derived biochar enhance perchlorate adsorption via hydrogen bonding to oxygen-containing organic groups. Environ. Sci. Technol. 48 (1), 279–288.
Fontecha-Camara, M.A., Lopez-Ramon, M.V., Alvarez-Merino, M.A., Moreno-Castilla, C., 2007. Effect of surface chemistry, solution pH, and ionic strength on the removal of herbicides diuron and amitrole from water by an activated carbon fiber. Langmuir 23 (3), 1242–1247.
Gao, J.A., Pedersen, J.A., 2005. Adsorption of sulfonamide antimicrobial agents to clay minerals. Environ. Sci. Technol. 39 (24), 9509–9516.
Gao, P.P., Mao, D.Q., Luo, Y., Wang, L.M., Xu, B.J., Xu, L., 2012a. Occurrence of sulfonamide and tetracycline-resistant bacteria and resistance genes in aquaculture environment. Water Res. 46 (7), 2355–2364.
Gao, Y.Q., Gao, N.Y., Deng, Y., Yang, Y.Q., Ma, Y., 2012b. Ultraviolet (UV) light-activated persulfate oxidation of sulfamethazine in water. Chem. Eng. J. 195, 248–253.
Gong, J.L., Wang, B., Zeng, G.M., Yang, C.P., Niu, C.G., Niu, Q.Y., Zhou, W.J., Liang, Y., 2009. Removal of cationic dyes from aqueous solution using magnetic multi-wall carbon nanotube nanocomposite as adsorbent. J. Hazard. Mater. 164 (2–3), 1517–1522.
Hale, S.E., Hanley, K., Lehmann, J., Zimmerman, A.R., Cornelissen, G., 2011. Effects of chemical, biological, and physical aging as well as soil addition on the sorption of pyrene to activated carbon and biochar. Environ. Sci. Technol. 45 (24), 10445–10453.
Hamscher, G., Pawelzick, H.T., Hoper, H., Nau, H., 2005. Different behavior of tetracyclines and sulfonamides in sandy soils after repeated fertilization with liquid manure. Environ. Toxicol. Chem. 24 (4), 861–868.
Hirsch, R., Ternes, T., Haberer, K., Kratz, K.L., 1999. Occurrence of antibiotics in the aquatic environment. Sci. Total Environ. 225 (1–2), 109–118.
Huang, D.L., Wang, R.Z., Liu, Y.G., Zeng, G.M., Lai, C., Xu, P., Lu, B.A., Xu, J.J., Wang, C., Huang, C., 2015. Application of molecularly imprinted polymers in wastewater treatment: a review. Environ. Sci. Pollut. Res. 22 (2), 963–977.
Huang, D.L., Zeng, G.M., Feng, C.L., Hu, S., Jiang, X.Y., Tang, L., Su, F.F., Zhang, Y., Zeng, W., Liu, H.L., 2008. Degradation of lead-contaminated lignocellulosic waste by phanerochaete chrysosporium and the reduction of lead toxicity. Environ. Sci. Technol. 42 (13), 4946–4951.
Huang, D.L., Zeng, G.M., Feng, C.L., Hu, S., Lai, C., Zhao, M.H., Su, F.F., Tang, L., Liu, H.L., 2010. Changes of microbial population structure related to lignin degradation during lignocellulosic waste composting. Bioresour. Technol. 101 (11), 4062–4067.
Inyang, M., Gao, B., Wu, L., Yao, Y., Zhang, M., Liu, L., 2013. Filtration of engineered nanoparticles in carbon-based fixed bed columns. Chem. Eng. J. 220, 221–227.
Inyang, M., Gao, B., Zimmerman, A., Zhang, M., Chen, H., 2014. Synthesis, characterization, and dye sorption ability of carbon nanotube-biochar nanocomposites. Chem. Eng. J. 236, 39–46.
Ji, L.L., Chen, W., Zheng, S.R., Xu, Z.Y., Zhu, D.Q., 2009. Adsorption of sulfonamide antibiotics to multiwalled carbon nanotubes. Langmuir 25 (19), 11608–11613.
Ji, L.L., Wan, Y.Q., Zheng, S.R., Zhu, D.Q., 2011. Adsorption of tetracycline and sulfamethoxazole on crop residue-derived ashes: implication for the relative importance of black carbon to soil sorption. Environ. Sci. Technol. 45 (13), 5580–5586.
Jones, D.L., Edwards-Jones, G., Murphy, D.V., 2011. Biochar mediated alterations in herbicide breakdown and leaching in soil. Soil Biol. Biochem. 43 (4), 804–813.
Kemper, N., 2008. Veterinary antibiotics in the aquatic and terrestrial environment. Ecol. Indic. 8 (1), 1–13.
Kim, S.C., Carlson, K., 2007. Temporal and spatial trends in the occurrence of human and veterinary antibiotics in aqueous and river sediment matrices. Environ. Sci. Technol. 41 (1), 50–57.
Lehmann, J., Joseph, S., 2009. Biochar for Environmental Management : Science and Technology. Earthscan, London; Sterling, VA, pp. 1–9.
Lertpaitoonpan, W., Ong, S.K., Moorman, T.B., 2009. Effect of organic carbon and pH on soil sorption of sulfamethazine. Chemosphere 76 (4), 558–564.
Lin, C.E., Lin, W.C., Chiou, W.C., Lin, E.C., Chang, C.C., 1996. Migration behavior and separation of sulfonamides in capillary zone electrophoresis. I. Influence of buffer pH and electrolyte modifier. J. Chromatogr. A 755 (2), 261–269.
Luo, W., Wang, B., Heron, C.G., Allen, M.J., Morre, J., Maier, C.S., Stickle, W.F., Ji, X.L., 2014. Pyrolysis of cellulose under ammonia leads to nitrogen-doped nanoporous carbon generated through methane formation. Nano Lett. 14 (4), 2225–2229.
Qiang, Z.M., Bao, X.L., Ben, W.W., 2013. MCM-48 modified magnetic mesoporous nanocomposite as an attractive adsorbent for the removal of sulfamethazine from water. Water Res. 47 (12), 4107–4114.
Rajapaksha, A.U., Vithanage, M., Ahmad, M., Seo, D.C., Cho, J.S., Lee, S.E., Lee, S.S., Ok, Y.S., 2015. Enhanced sulfamethazine removal by steam-activated invasive plant-derived biochar. J. Hazard. Mater. 290, 43–50.
Rajapaksha, A.U., Vithanage, M., Zhang, M., Ahmad, M., Mohan, D., Chang, S.X., Ok, Y.S., 2014. Pyrolysis condition affected sulfamethazine sorption by tea waste biochars. Bioresour. Technol. 166, 303–308.
Schoen, D.T., Schoen, A.P., Hu, L.B., Kim, H.S., Heilshorn, S.C., Cui, Y., 2010. High speed water sterilization using one-dimensional nanostructures. Nano Lett. 10 (9), 3628–3632.
Shawky, H.A., El-Aassar, A.H.M., Abo-Zeid, D.E., 2012. Chitosan/carbon nanotube composite beads: preparation, characterization, and cost evaluation for mercury removal from wastewater of some industrial cities in Egypt. J. Appl. Polym. Sci. 125, E93–E101.
Sparrevik, M., Lindhjem, H., Andria, V., Fet, A.M., Cornelissen, G., 2014. Environmental and socioeconomic impacts of utilizing waste for biochar in rural areas in Indonesia-A systems perspective. Environ. Sci. Technol. 48 (9), 4664–4671.
Tan, X.F., Liu, Y.G., Zeng, G.M., Wang, X., Hu, X.J., Gu, Y.L., Yang, Z.Z., 2015. Application of biochar for the removal of pollutants from aqueous solutions. Chemosphere 125, 70–85.
Tang, J.C., Lv, H.H., Gong, Y.Y., Huang, Y., 2015. Preparation and characterization of a novel graphene/biochar composite for aqueous phenanthrene and mercury removal. Bioresour. Technol. 196, 355–363.
Tang, W.W., Zeng, G.M., Gong, J.L., Liang, J., Xu, P., Zhang, C., Huang, B.B., 2014. Impact of humic/fulvic acid on the removal of heavy metals from aqueous solutions using nanomaterials: a review. Sci. Total Environ. 468, 1014–1027.
Teixido, M., Hurtado, C., Pignatello, J.J., Beltran, J.L., Granados, M., Peccia, J., 2013. Predicting contaminant adsorption in black carbon (Biochar)-Amended soil for the veterinary antimicrobial sulfamethazine. Environ. Sci. Technol. 47 (12), 6197–6205.
Teixido, M., Pignatello, J.J., Beltran, J.L., Granados, M., Peccia, J., 2011. Speciation of the ionizable antibiotic sulfamethazine on black carbon (biochar). Environ. Sci. Technol. 45 (23), 10020–10027.
Titirici, M.M., White, R.J., Brun, N., Budarin, V.L., Su, D.S., del Monte, F., Clark, J.H., MacLachlan, M.J., 2015. Sustainable carbon materials. Chem. Soc. Rev. 44 (1), 250–290.
Titirici, M.M., White, R.J., Falco, C., Sevilla, M., 2012. Black perspectives for a green future: hydrothermal carbons for environment protection and energy storage. Energy & Environ. Sci. 5 (5), 6796–6822.
Trakal, L., Veselska, V., Safarik, I., Vitkova, M., Cihalova, S., Komarek, M., 2016. Lead and cadmium sorption mechanisms on magnetically modified biochars. Bioresour. Technol. 203, 318–324.
Vinu, A., Hossain, K.Z., Kumar, G.S., Ariga, K., 2006. Adsorption of L-histidine over mesoporous carbon molecular sieves. Carbon 44 (3), 530–536.
Wang, S., Zhang, H.Y., Wang, L., Duan, Z.J., Kennedy, I., 2006. Analysis of sulphonamide residues in edible animal products: a review. Food Addit. Contam. 23 (4), 362–384.
Wang, X.L., Tao, S., Xing, B.S., 2009. Sorption and competition of aromatic compounds and humic acid on multiwalled carbon nanotubes. Environ. Sci. Technol. 43 (16), 6214–6219.
Wu, Z.B., Zhong, H., Yuan, X.Z., Wang, H., Wang, L.L., Chen, X.H., Zeng, G.M., Wu, Y., 2014. Adsorptive removal of methylene blue by rhamnolipid-functionalized graphene oxide from wastewater. Water Res. 67, 330–344.
Xu, P., Zeng, G.M., Huang, D.L., Feng, C.L., Hu, S., Zhao, M.H., Lai, C., Wei, Z., Huang, C., Xie, G.X., Liu, Z.F., 2012. Use of iron oxide nanomaterials in wastewater treatment: a review. Sci. Total Environ. 424, 1–10.
Xu, W.H., Zhang, G., Li, X.D., Zou, S.C., Li, P., Hu, Z.H., Li, J., 2007. Occurrence and elimination of antibiotics at four sewage treatment plants in the Pearl River Delta (PRD), South China. Water Res. 41 (19), 4526–4534.
Yan, Y.B., Miao, J.W., Yang, Z.H., Xiao, F.X., Yang, H.B., Liu, B., Yang, Y.H., 2015. Carbon nanotube catalysts: recent advances in synthesis, characterization and applications. Chem. Soc. Rev. 44 (10), 3295–3346.
Yang, Q.Q., Chen, G.C., Zhang, J.F., Li, H.L., 2015. Adsorption of sulfamethazine by multi-walled carbon nanotubes: effects of aqueous solution chemistry. Rsc Adv. 5 (32), 25541–25549.
Yang, Y.N., Sheng, G.Y., 2003. Pesticide adsorptivity of aged particulate matter arising from crop residue burns. J. Agric. Food Chem. 51 (17), 5047–5051.
Zeng, G.M., Chen, M., Zeng, Z.T., 2013a. Risks of neonicotinoid pesticides. Science 340 (6139), 1403–1403.
Zeng, G.M., Chen, M., Zeng, Z.T., 2013b. Shale gas: surface water also at risk. Nature 499 (7457), 154–154.
Zhang, C., Liu, L., Zeng, G.M., Huang, D.L., Lai, C., Huang, C., Wei, Z., Li, N.J., Xu, P., Cheng, M., Li, F.L., He, X.X., Lai, M.Y., He, Y.B., 2014a. Utilization of nano-gold tracing technique: study the adsorption and transmission of laccase in mediator-involved enzymatic degradation of lignin during solid-state fermentation. Biochem. Eng. J. 91, 149–156.
Zhang, C., Zeng, G.M., Huang, D.L., Lai, C., Huang, C., Li, N.J., Xu, P., Cheng, M., Zhou, Y.Y., Tang, W.W., He, X.X., 2014b. Combined removal of di(2-ethylhexyl) phthalate (DEHP) and Pb(II) by using a cutinase loaded nanoporous gold-polyethyleneimine adsorbent. Rsc Adv. 4 (98), 55511–55518.
Zhang, D., Pan, B., Zhang, H., Ning, P., Xing, B.S., 2010. Contribution of different sulfamethoxazole species to their overall adsorption on functionalized carbon nanotubes. Environ. Sci. Technol. 44, 3806–3811.
Zhang, M., Gao, B., Yao, Y., Xue, Y.W., Inyang, M., 2012. Synthesis, characterization, and environmental implications of graphene-coated biochar. Sci. Total Environ. 435, 567–572.